

Applications of a Consistent Grayscale-free Topology Optimization Method to Industrial Design Problems

Shintaro Yamasaki¹, Atsushi Kawamoto², Tsuyoshi Nomura³, Kikuo Fujita⁴

¹ Osaka University, Suita, Japan, yamasaki@mech.eng.osaka-u.ac.jp

² Toyota Central R&D Labs., Inc., Nagakute, Japan, atskmt@mosk.tytlabs.co.jp

³ Toyota Central R&D Labs., Inc., Nagakute, Japan, nomu2@mosk.tytlabs.co.jp

⁴ Osaka University, Suita, Japan, fujita@mech.eng.osaka-u.ac.jp

1. Abstract

In a previous research, we proposed a consistent grayscale-free topology optimization method using the level-set method and zero-level boundary tracking mesh. In this method, the shape and topology of the design target are represented using the level-set method and the state variables are computed using a mesh tracking the zero iso-contour of the level-set function, which we call the zero-level boundary. Because of the characteristics of the level-set method and zero-level boundary tracking mesh, essentially grayscale-free representation is achieved. Furthermore, a double-well potential based regularization technique is employed in the proposed method to regularize the structural optimization problem. Because of these enhancements, we realize essentially grayscale-free topology optimization where the design variables are updated on the basis of the standard framework of mathematical programming. In the present research, we apply the proposed grayscale-free topology optimization method to several structural optimization problems in industry, such as the minimum compliance and invehicle reactor design problems. Through the application to these design problems, we investigate the potential of the proposed grayscale-free topology optimization method.

2. Keywords: Topology optimization, Level-set method, Grayscale-free method, Design problem

3. Introduction

Topology optimization is a design approach for yielding superior structural designs while considering the shape and topology. There are two basic ideas in topology optimization: one is replacing the original structural design problem with a material distribution problem in a given design domain, and the other is updating the design variables representing material distribution by using mathematical programming. Because of mathematical programming, it is expected that the optimal solution, i.e., the optimal structure, is obtained.

While homogenization or density based topology optimization [1, 2] has achieved great success, topology optimization based on the level-set method has recently gained attention from many researchers. The level-set method [3] is a shape representation method for different two phases; the distribution of these two phases is represented by the sign of a scalar function called the level-set function. On the basis of this shape representation method, the material distribution of the target structure is represented using the level-set function in level-set based topology optimization [4, 5, 6].

Because the structural boundary is always clearly represented by the level-set method, grayscale elements seems to be suppressed in level-set based topology optimization. This is a great advantage when comparing with homogenization or density based topology optimization. However, grayscale elements cannot be completely suppressed even in level-set based topology optimization when the state variables are computed using a fixed mesh such as the Eulerian mesh for maintaining the level-set function. To realize completely grayscale-free topology optimization, we have proposed a level-set based topology optimization method [7]. In the proposed method, the shape and topology of the design target are represented using the level-set function, and the state variables are computed using a mesh that conforms to the structural boundary, i.e., the zero iso-contour of the level-set function.

In this paper, we further investigate the usefulness of the proposed method by applying it to several design problems, concretely, the minimum compliance problem and an invehicle reactor design problem. In Section 4, we briefly explain the grayscale-free topology optimization method that we previously proposed. In Section 5, we discuss how apply the proposed method to the two design problems. In Section 6, we provide several numerical examples to confirm the validity of the applications. Finally, we conclude the discussion in Section 7.

4. Proposed Grayscale-free Topology Optimization Method

In this section, we briefly explain the grayscale-free topology optimization method proposed in Reference [7].

4.1. Shape Representation Based on the Level-set Method

In the proposed method, the shape and topology of the target structure are represented using the level-set function $\phi(\mathbf{x})$, which is defined as

$$\begin{aligned}\phi(\mathbf{x}) &> 0 && \text{for } \forall \mathbf{x} \in \Omega \setminus (\partial\Omega \setminus \partial D), \\ \phi(\mathbf{x}) &= 0 && \text{for } \forall \mathbf{x} \in \partial\Omega \setminus \partial D, \\ \phi(\mathbf{x}) &< 0 && \text{for } \forall \mathbf{x} \in D \setminus \Omega,\end{aligned}\tag{1}$$

where D is the design domain, Ω is the material domain, ∂D and $\partial\Omega$ are, respectively, the boundaries of D and Ω , and \mathbf{x} is a position in D . Furthermore, the smoothness of ϕ is ensured by solving the following equation [8]:

$$-R^2 \nabla^2 \phi + \phi = \psi \quad \text{in } D, \quad \frac{\partial \phi}{\partial \mathbf{n}} = 0 \quad \text{on } \partial D,\tag{2}$$

where ψ is a function that governs ϕ , and R is the length scale parameter.

In the implementation, ϕ and ψ are discretized using the Eulerian mesh, and the discretized ϕ and ψ are represented by the respective nodal value vectors Φ and Ψ . Ψ are the design variables in the proposed method, and these are bounded as follows:

$$-1 \leq \Psi_i \leq 1 \quad \text{for } i = 1, \dots, n_{\text{psi}}\tag{3}$$

where Ψ_i is the i th component of Ψ and n_{psi} is the component number of Ψ .

4.2. State Variable Computation Using the Zero-level Boundary Tracking Mesh

As explained in Section 4.1, the material domain Ω is represented by Φ in the discrete system. Then, the Eulerian mesh that maintains Φ does not conform to the zero iso-contour of the level-set function (hereafter, we call it the zero-level boundary) in usual cases. Therefore, grayscale elements are yielded around the zero-level boundary when the state variables are computed using the Eulerian mesh. To completely suppress such grayscale elements, a mesh that accurately tracks the zero-level boundary is generated at every optimization iteration in the proposed method. This zero-level boundary tracking mesh is generated by moving the nodes of the Eulerian mesh, and used to compute the state variables. For the details of the mesh generation procedure, see Reference [7].

4.3. Sensitivity Analysis

In the proposed method, it is assumed that the objective and constraint functions are computed using the zero-level boundary tracking mesh. On the other hand, the nodal level-set functions Φ are maintained at each node of the Eulerian mesh. Therefore, the relationship of sensitivities between the Eulerian and zero-level boundary tracking meshes should be known to derive the sensitivities with respect to Φ . Fortunately, this relationship has been clearly given in Reference [7], therefore, the sensitivities with respect to Φ can be successfully derived if the sensitivities with respect to the nodal coordinates of the zero-level boundary tracking mesh. Furthermore, the sensitivities with respect to the design variables, i.e., Ψ can be clearly derived using the sensitivities with respect to Φ as shown in Reference [7].

As a result, the sensitivities with respect to the design variables are derived using the framework proposed in Reference [7], if the sensitivities with respect to the nodal coordinates of the zero-level boundary tracking mesh are derived.

4.4. Double-well Potential Based Regularization

In the proposed method, a double-well potential based regularization technique is used to regularize the structural optimization problem. That is, the structural optimization problem is formulated as follows:

$$\begin{aligned}\underset{\Psi}{\text{minimize}} \quad & f_0 + w f_{\text{reg}}, \\ \text{subject to} \quad & f_i \leq f_{i \max}, \quad \text{for } i = 1, \dots, n_{\text{cns}},\end{aligned}\tag{4}$$

where f_0 is the original objective function, f_i and $f_{i \max}$ are, respectively, the i th constraint function and the corresponding allowable upper limit, n_{cns} is the number of constraints, and w is the weighting coefficient. f_{reg} is the double-well potential based regularization term that is computed with the Eulerian mesh as follows:

$$f_{\text{reg}} = \bigcup_{e=1}^{n_D} \int_{V^e} \left((\phi^*)^2 - 1 \right)^2 dv,\tag{5}$$

where $\int_{V^e} dv$ represents the volume integral in an element, ϕ^* is the level-set function in that element, and $\bigcup_{e=1}^{n_D}$ represents the union set of the elements in D . Because of the regularization term f_{reg} , the level-set function tends

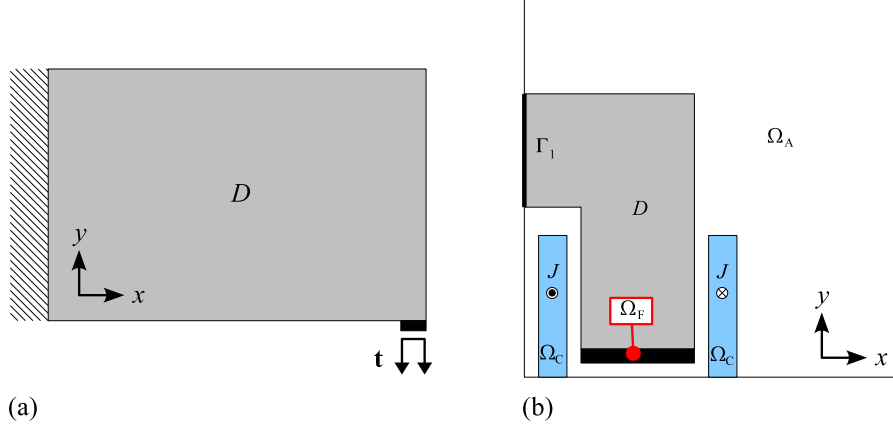


Figure 1: Analysis models: (a) minimum compliance problem; and (b) invehicle reactor design problem.

to move 1 or -1 except around the zero-level boundary.

4.5. Optimization Flow

On the basis of the discussions in Sections 4.1, 4.2, 4.3, and 4.4, the optimization flow of the proposed method is described as follows:

- (i) Provide an Eulerian mesh and initialize the design variables Ψ .
- (ii) Compute the nodal level-set functions, i.e., Φ , by solving Equation (2) in the discrete system.
- (iii) Generate the zero-level boundary tracking mesh as explained in Section 4.2.
- (iv) Compute f_i with the zero-level boundary tracking mesh while computing f_{reg} with the Eulerian mesh.
- (v) Terminate the optimization successfully if the termination condition is satisfied.
- (vi) Compute the sensitivities with respect to Φ and Ψ as explained in Section 4.3.
- (vii) Update the design variables using nonlinear programming to solve the optimization problem formulated in Equation (4), and return to (ii).

Note that, the proposed method assumes the Eulerian mesh consisting of linear triangular elements because of the mesh generation procedure.

As explained in Section 4.3, the sensitivities with respect to the nodal coordinates of the zero-level boundary tracking mesh must be derived for applying the proposed method to respective structural design problems. We derive them in the next section.

5. Applications to Several Design Problems

5.1. Minimum Compliance Problem

In the minimum compliance problem, we assume a two-dimensional analysis model shown in Figure 1(a). As shown in this figure, the design domain D is displayed in gray, a surface load \mathbf{t} is applied in a part of the boundary, and the displacement is fixed on a part of the boundary. Then, our objective is minimizing the mean compliance while constraining the volume of the structure. That is, f_0 and f_1 in Equation (4) are computed with the zero-level boundary tracking mesh as follows:

$$f_0 = \mathbf{U}^T \mathbf{T}, \quad (6)$$

$$f_1 = \bigcup_{e=1}^{n_\Omega} \int_{V^e} dv, \quad (7)$$

where $\bigcup_{e=1}^{n_\Omega}$ represents the union set of the elements in Ω , \mathbf{U} and \mathbf{T} are, respectively, the discretized displacement field and surface load. Furthermore, \mathbf{U} is computed by solving the following equation:

$$\mathbf{T} - \mathbf{K}\mathbf{U} = \mathbf{0}, \quad (8)$$

where \mathbf{K} is the total stiffness matrix.

From Equations (6) and (8), we obtain

$$f_0 = \mathbf{U}^\top \mathbf{T} + \mathbf{V}^\top \{\mathbf{T} - \mathbf{K}\mathbf{U}\}, \quad (9)$$

where \mathbf{V} is the adjoint variable vector. Therefore, the sensitivities of f_0 with respect to the nodal coordinates of the zero-level boundary tracking mesh are derived as follows:

$$\frac{\partial f_0}{\partial X_i} = \left\{ \frac{\partial \mathbf{U}}{\partial X_i} \right\}^\top \mathbf{T} + \mathbf{V}^\top \left\{ -\frac{\partial \mathbf{K}}{\partial X_i} \mathbf{U} - \mathbf{K} \frac{\partial \mathbf{U}}{\partial X_i} \right\} = -\mathbf{V}^\top \frac{\partial \mathbf{K}}{\partial X_i} \mathbf{U}, \quad (10)$$

where X_i is the x coordinate of the i th node of the zero-level boundary tracking mesh, and \mathbf{V} is the solution of the following adjoint equation:

$$\mathbf{T} - \mathbf{K}^\top \mathbf{V} = \mathbf{0}. \quad (11)$$

By denoting the y coordinate of the i th node as Y_i , the corresponding sensitivity is similarly derived as

$$\frac{\partial f_0}{\partial Y_i} = -\mathbf{V}^\top \frac{\partial \mathbf{K}}{\partial Y_i} \mathbf{U}. \quad (12)$$

The sensitivities of f_1 with respect to the nodal coordinates of the zero-level boundary tracking mesh are simply derived as

$$\frac{\partial f_1}{\partial X_i} = \frac{\partial}{\partial X_i} \left\{ \bigcup_{e=1}^{n_\Omega} \int_{V_e} dv \right\}, \quad \frac{\partial f_1}{\partial Y_i} = \frac{\partial}{\partial Y_i} \left\{ \bigcup_{e=1}^{n_\Omega} \int_{V_e} dv \right\}. \quad (13)$$

By incorporating Equations (10), (12), and (13) into the topology optimization method explained in Section 4, we can obtain the optimized structure that minimizes the mean compliance.

5.2. Invehicle Reactor Design Problem

Invehicle reactor is a component of the DC-DC converter, which is used in hybrid and electric vehicles. Because the invehicle reactor contributes to performances of those vehicles, it is important to design superior invehicle reactors. In this paper, we assume a two-dimensional analysis model shown in Figure 1(b). This analysis model is a quarter model where the left and bottom edges are the symmetric boundaries. Ω_A is the domain filled with air, Ω_F is the domain filled with ferrite, Ω_C represents coils, and D is the design domain where ferrite and air are distributed. Electric current density J is imposed in the coil domains Ω_C .

Here, our objective is minimizing the eddy-current loss in the coils while maintaining sufficient inductance. Then, f_0 and f_1 in Equation (4) are given as follows:

$$f_0 = \mathbf{A}^\top \mathbf{F} \mathbf{A}, \quad (14)$$

$$f_1 = \mathbf{A}^\top \mathbf{G}, \quad (15)$$

where \mathbf{A} is the discretized magnetic potential for computing the magnetic flux density (B_x, B_y) , \mathbf{F} is the matrix for integrating $B_x^2 + B_y^2$ in Ω_C , and \mathbf{G} is the vector for integrating B_y on Γ_1 . \mathbf{A} is computed by solving the following equation:

$$\mathbf{H} \mathbf{A} + \mathbf{L} = \mathbf{0}, \quad (16)$$

where \mathbf{H} is the magnetic stiffness matrix and \mathbf{L} is the vector representing the imposed current. From Equations (14) and (16), the sensitivity of f_0 with respect to X_i is derived as

$$\begin{aligned} \frac{\partial f_0}{\partial X_i} &= \left\{ \frac{\partial \mathbf{A}}{\partial X_i} \right\}^\top \mathbf{F} \mathbf{A} + \mathbf{A}^\top \mathbf{F} \frac{\partial \mathbf{A}}{\partial X_i} + \mathbf{V}_1^\top \left\{ \mathbf{H} \frac{\partial \mathbf{A}}{\partial X_i} + \frac{\partial \mathbf{H}}{\partial X_i} \mathbf{A} \right\} \\ &= \left\{ \frac{\partial \mathbf{A}}{\partial X_i} \right\}^\top \left\{ \mathbf{F} \mathbf{A} + \mathbf{F}^\top \mathbf{A} + \mathbf{H}^\top \mathbf{V}_1 \right\} + \mathbf{V}_1^\top \frac{\partial \mathbf{H}}{\partial X_i} \mathbf{A} \\ &= \mathbf{V}_1^\top \frac{\partial \mathbf{H}}{\partial X_i} \mathbf{A}, \end{aligned} \quad (17)$$

where the adjoint variable vector \mathbf{V}_1 is obtained by solving the following adjoint equation:

$$\mathbf{F} \mathbf{A} + \mathbf{F}^\top \mathbf{A} + \mathbf{H}^\top \mathbf{V}_1 = \mathbf{0}. \quad (18)$$

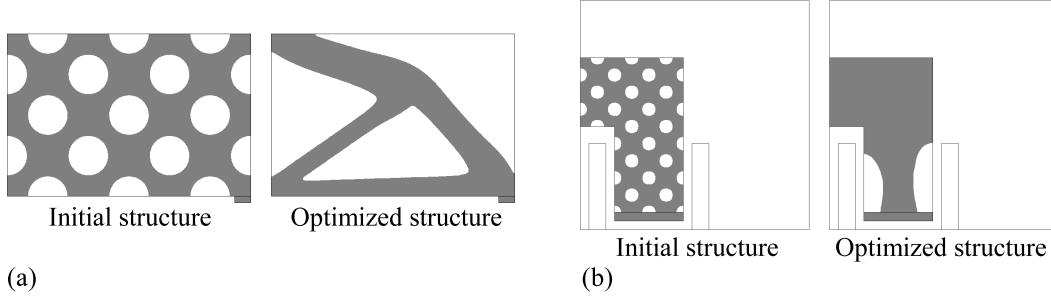


Figure 2: Initial and Optimized structures: (a) minimum compliance problem; and (b) invehicle reactor design problem.

Similarly, the sensitivity of f_0 with respect to Y_i is derived as

$$\frac{\partial f_0}{\partial Y_i} = \mathbf{V}_1^\top \frac{\partial \mathbf{H}}{\partial Y_i} \mathbf{A}. \quad (19)$$

From Equations (15) and (16), the sensitivities of f_1 with respect to X_i and Y_i are derived as

$$\frac{\partial f_1}{\partial X_i} = \mathbf{V}_2^\top \frac{\partial \mathbf{H}}{\partial X_i} \mathbf{A}, \quad \frac{\partial f_1}{\partial Y_i} = \mathbf{V}_2^\top \frac{\partial \mathbf{H}}{\partial Y_i} \mathbf{A}, \quad (20)$$

where the adjoint variable vector \mathbf{V}_2 is obtained by solving the following adjoint equation:

$$\mathbf{G} + \mathbf{H}^\top \mathbf{V}_2 = \mathbf{0}. \quad (21)$$

In the same manner as the minimum compliance problem, we can obtain optimized invehicle reactors by incorporating Equations (17), (19), and (20) into the topology optimization method explained in Section 4.

6. Numerical Examples

In this section, we provide two numerical examples for the minimum compliance and invehicle reactor design problems. First, we consider the analysis domain shown in Figure 1(a) for the minimum compliance problem. Its total size is 0.75×0.5 and it is discretized with triangular elements whose maximum length is 0.005. The young's modulus and poisson's ratio of the structural material are set to 1 and 0.3, respectively. The surface load \mathbf{t} is set to $(0, -0.01)$. The parameter R in Equation (2) is set to 0.01. The maximum allowable volume, i.e., $f_{1 \max}$, is set to 0.15. The optimizer is sequential linear programming (SLP) and its move limit is set to 0.05. On the above problem settings, we provide the initial structure shown in Figure 2(a), and as a result of optimization, we obtain the optimized structure shown in Figure 2(a) at iteration 493. Because the obtained optimized structure is very similar to optimized structures obtained in many relevant studies, we consider that the application to the minimum compliance problem is successfully achieved.

Next, we consider the analysis domain shown in Figure 1(b) for the invehicle reactor design problem. Its total size is $0.08\text{m} \times 0.08\text{m}$ and it is discretized with triangular elements whose maximum length is 0.001m. The relative permeability of ferrite is set to 150. The electric current density in the coils, i.e., J , is set to $3 \times 10^6 \frac{\text{A}}{\text{m}^2}$. The parameter R in Equation (2) is set to 0.002m. $f_{1 \max}$ is set to $-0.058\text{T} \cdot \text{m}$, that is, the minimum allowable magnetic flux through Γ_1 is set to $0.058\text{T} \cdot \text{m}$. The optimizer is SLP and its move limit is set to 0.05. On the above problem settings, we provide the initial structure shown in Figure 2(b), and as a result of optimization, we obtain the optimized structure shown in Figure 2(b) at iteration 109. Note that, ferrite distribution is displayed in gray in Figure 2(b). As shown in Figure 2(b), left and right bottom parts are clipped in the optimized structure. By eliminating ferrite in neighborhood of the coil domains Ω_C , leakage flux in Ω_C can be effectively decreased. Furthermore, such elimination does not deteriorate the inductance so much. Because physically appropriate ferrite distribution is obtained, we consider that the application to the invehicle reactor design problem is also successfully achieved.

7. Conclusion

In this paper, we applied our previously proposed method to the minimum compliance and invehicle reactor design problems. Our previously proposed method is a consistent grayscale-free topology optimization method and it is

promising because of its grayscale-free property. Furthermore, because the optimization framework has already been established, only the nodal coordinate sensitivities of the objective and constraint functions are required when applying our previously proposed method to design problems in industry. To demonstrate the potential of our previously proposed method, we investigated two applications, i.e., the applications to the minimum compliance and invehicle reactor design problems. Especially, the invehicle reactor design problem is important in an industrial view point because it is a great objective in industry to realize high performance hybrid and electric vehicles. As shown in the numerical examples, physically valid optimized structures were obtained in both two design problems, therefore, we consider that the applications to these design problems are successfully achieved. In future works, we will investigate applications to further design problems in industry and propose functional structures which have superior performances.

8. References

- [1] M. P. Bendsøe and N. Kikuchi. Generating optimal topologies in structural design using a homogenization method. *Computer Methods in Applied Mechanics and Engineering*, 71(2):197–224, November 1988.
- [2] M. P. Bendsøe. Optimal shape design as a material distribution problem. *Structural Optimization*, 1(4):193–202, 1989.
- [3] S. Osher and J. A. Sethian. Fronts propagating with curvature-dependent speed: Algorithms based on Hamilton-Jacobi formulations. *Journal of Computational Physics*, 78(1):12–49, November 1988.
- [4] J. A. Sethian and A. Wiegmann. Structural boundary design via level-set and immersed interface methods. *Journal of Computational Physics*, 163(2):489–528, September 2000.
- [5] M. Y. Wang, X. Wang, and D. Guo. A level set method for structural topology optimization. *Computer Methods in Applied Mechanics and Engineering*, 192(1–2):227–246, 2003.
- [6] G. Allaire, F. Jouve, and A. M. Toader. Structural optimization using sensitivity analysis and a level-set method. *Journal of Computational Physics*, 194(1):363–393, February 2004.
- [7] S. Yamasaki, A. Kawamoto, T. Nomura, and K. Fujita. A consistent grayscale-free topology optimization method using the level-set method and zero-level boundary tracking mesh. *International Journal for Numerical Methods in Engineering*, 101(10):744–773, March 2015.
- [8] A. Kawamoto, T. Matsumori, S. Yamasaki, T. Nomura, T. Kondoh, and S. Nishiwaki. Heaviside projection based topology optimization by a PDE-filtered scalar function. *Structural and Multidisciplinary Optimization*, 44(1):19–24, July 2011.